International Journal of Pure and Applied Mathematics
Volume 117 No. 20 2017, 359-374
ISSN: 1311-8080 (printed version); ISSN: 1314-3395 (on-line version)
url: http://www.ijpam.eu
Special Issue

ijpam.eu

A Study on Hybrid Generation Control System Using Smart Control

Hee Chul, Kim
Dept. of Computer Engineering, 277 Hyodeok-ro,
Gwangju University, Nam-gu Gwangju city, Korea.
jaziri@daum.net

Abstract

This study was conducted to investigate the effect of the (EDLC: Electric Double Layer Capacitor)It is aiming to apply the lighting device using LED light source as the load of solar-wind power hybrid power generation system for independent power source and to develop the street light system device with high output power generation system. Stand-alone photovoltaic power generation system is independent of Korean power system and operates independently. Therefore, it is simple and low cost construction equipment. However, converter including(MPPT: Maximum Power Point Tracking). A battery charging circuit and a battery management circuit are required. Hybrid power generation combines a plurality of systems having different characteristics to construct a power generation system complementary to each other, so that a plurality of systems can be smoothly combined, and advantages of each individual system and further advantages. The purpose is to acquire. Solar power and wind power generation are relative to each other. In sunny weather, wind power was found to increase in the windy cloudy weather. If such hybrid type of power is produced, it is possible to reduce the pulsation of the total production power, so that it can supply stable power to the load system.

Key Words:MPPT, Efficiency, charge, solar-wind hybrid generation, standalone.

1. Introduction

In order to enhance the utilization of renewable energy for the commercialization of solar-wind power hybrid power generation system using street lighting for EDLC and to secure a stable mechanism for energy production and storage, it is necessary to utilize consistent energy from the energy source.

Stand-alone photovoltaic power generation system is independent of Korean power system and operates independently. Therefore, it is simple and low cost construction equipment. However, converter including Maximum Power Point Tracking (MPPT) A battery charging circuit and a battery management circuit are required.

It is aimed to develop a streetlight system device with a high power generation system by applying a lighting device using an LED light source as a load of a solar-wind power hybrid power generation system for an independent power source.

The composition of this paper is as follows. In Section 2, the system configuration is presented. In Section 3, the structural design technology for the stability of PV-wind power hybrid power generation system using EDLC is secured. In Section 4, the drive design technique of constant current and constant voltage is applied. Finally, Chapter 5 concludes the paper and concludes with future research proposals.

2. Related Works

Power generation facilities for independent power sources are mainly operated by solar power generation systems.Solar power generation systems are directly influenced by the weather, which causes many problems in power generation during the summer rainy season.Figure 1 shows that the array of solar cells and the direct current generated from the wind power generator are converted into alternating current through the inverter to supply the power to the general load and the surplus power to the battery[1].

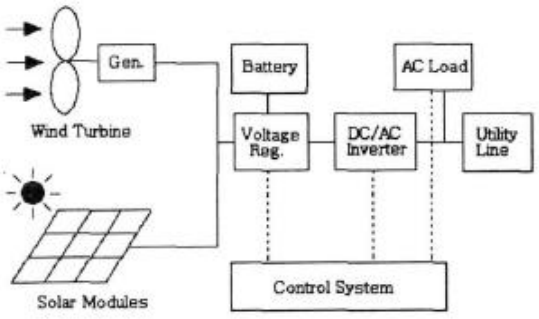

Figure 1: Energy Storage Flow Diagram of a Hybrid Power Generation System

Principles of Wind Power Generation

It is a technology that supplies induction electricity generated by turning wind force to rotational force to power system or consumer, and it has characteristics of energy source which is temporary and changeable.Wind power converts the wind force into rotational force, which is transmitted to the generator through a power transmission device.

The power generated from the generator is transferred to the power system in the case of the grid-connected type through a proper type of power conversion process, and is delivered to the final consumer in the case of the stand-alone type. [2].

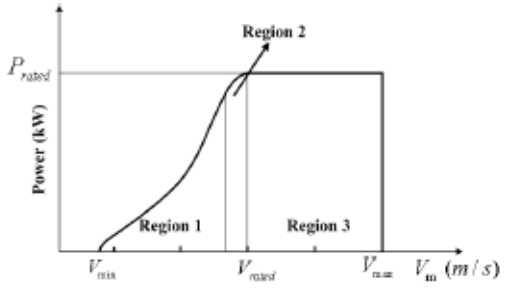

Figure 2: Wind Turbine Power Curve

Figure 2 shows the power curve of the wind turbine divided into region 1 (low wind speed), region 2 (transition region), and region 3 (high wind speed).In region 1, the blade pitch control is not performed, but the blade is driven at a fixed optimum pitch angle in the design of the blade, and the generator is controlled by the maximum output point tracking (MPPT) method to extract the maximum out-put.Zone3 performs generator torque control to prevent the rotational speed and output of the wind turbine from exceeding the allowable limits. [3].

Energy Generation in Wind Power Systems

Generators generate electrical energy by the characteristics of a wind turbine, a powertrain that is converted to mechanical energy by the wind.The kinetic energy of the fluid when the velocity of the air with mass m [kg] is V [m / s] is shown in Eq. (1).

$$E\omega = \frac{1}{2}\, mV^2[joules] \quad (1)$$

In this case, the volume V of a part of the air flow (A) is expressed by A (m^2) and the thickness of the parcel is D (2).

$$\mathrm{V} = \mathrm{AD}[m^3\,] \quad (2)$$

Assuming that the parcel of thickness D of air passes through time T, velocity v is given by equation (3).

$$v = \frac{D}{T}[m/s] \tag{3}$$

Therefore, the wind force of the air is given by Eq. (4).

$$P_{air} = \frac{1}{2}(mass\ flowrate\ per\ second)V^2\omega \tag{4}$$

$$= \frac{1}{2}(\rho ADV_\omega)V_\omega^2$$

$$= \frac{1}{2}\rho ATV_\omega^3[W]$$

$$= 0.5\rho AT(V_\omega)^3C_p[W]$$

Where ρ (kg / ㎥) is the air density, (m / s) is the wind speed, and A (㎡) is the area of the turbine blade moving, ie the rotating cross section of the wind turbine, Depends on the operating state of the generator. Equation (2) is the ideal wind force that can be generated by wind speed. The energy output from the rotor due to wind power is given by Eq. (5).

$$P = \frac{E\omega}{T} = \frac{\frac{1}{2}\rho \cdot V^3 \cdot A \cdot T}{T} = \frac{1}{2}\rho \cdot V^3 \cdot A \tag{5}$$

Here, the energy output and the cross-sectional area of the rotor are summarized in Equation (6).

$$\frac{P}{A} = \frac{1}{2}\rho \cdot V^3 \tag{6}$$

Figure 3 shows the relationship between wind speed and wind force.

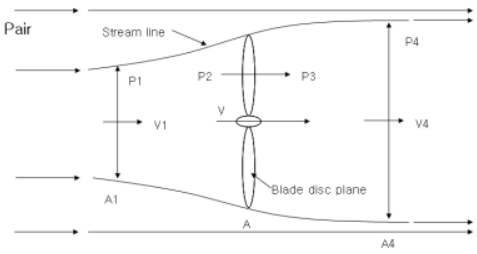

Figure 3: Fluid Flow Type

In Fig. 3, the force T applied to the rotor is the same as the change in the input / output momentum.

$$T = m(V_1 - V_4) = \rho AV(V_1 - V_4) \tag{7}$$

From the pressure condition, the force T is given by Eq. (8).

$$T = A(P_2 - P_3) \tag{8}$$

When Bernoulli's equation is applied to the rotor phase and the downstream phase, the equations (9) and (10) are used.

$$\frac{1}{2}\rho V_1^2 + P_1 = \frac{1}{2}\rho V^2 + P_2 \tag{9}$$

$$\frac{1}{2}\rho V_{\alpha}^{2} + P_{\alpha} = \frac{1}{2}\rho V^{2} + P_{s} \quad (10)$$

Therefore, subtracting Eq. (10) from Eq. (9) yields Eq. (11).

$$P_{z} - P_{s} = \frac{1}{2}\rho(V_{1}^{2} - V_{4}^{2}) \quad (11)$$

Where p1 and p2 are the same in the free stream. Equation (11) is substituted into Equation (8), and equation (12) is obtained.

$$\mathrm{T} = \frac{1}{2}\rho A(V_{1}^{2} - V_{4}^{2}) \quad (12)$$

Substituting Eq. (12) into Eq. (7) for input and output momentum is equivalent to Eq. (13).

$$\mathrm{V} = \frac{1}{2}(V_{1} - V_{4}) \quad (13)$$

The axial induction factor $V = V_{1}(1-a)$ If you define $V_{4} = V_{1}(1-2a)$ The kinetic energy obtained from the rotor is given by Eq. (14).

$$\mathrm{P} = 2\rho \mathrm{A} V_{1}^{3} \cdot \alpha(1-\alpha)^{2} \quad (14)$$

The maximum output is $dP/da = 0$ the value of a is $\frac{1}{3}$. Therefore, Equation (15) is obtained.

$$\mathrm{P}_{max} = 0.593 \times \left(\frac{1}{2}\rho A V_{1}^{3}\right) \quad (15)$$

At this time, 0.593 is the coefficient of Betz. The maximum power is a value that can be generated based on this, but actually Betz has a coefficient less than 0.5.the electrical energy that a wind power system can obtain from wind energy encompasses not only the power factor of the rotor, but also the efficiency of the transmission device and the efficiency of the generator to deliver the mechanical energy generated by the rotor. Therefore, the electrical output P (V) of the wind turbine that can be obtained from the wind is expressed by Eq. (16)[4].

$$\mathrm{P(V)} = \frac{1}{2}\rho A V^{3} \cdot C_{\alpha} \cdot \eta_{m} \cdot \eta_{\tau} \quad (16)$$

Is given by the curve of the power factor and the tip-speed ratio of the wind turbine. Also, the ratio of the state is given by Eq. (17).

$$\lambda = \frac{\omega_{m} R}{V} \quad (17)$$

Where is the radius of the wind turbine rotor and (rad / s) is the rotational angular velocity. Figure 4 shows the change in output P with changes in wind speed. Pure wind energy is expressed as a curve proportional to the third power of the wind speed, and is the product of 0.593 times the curve of the energy generated in the rotor of the ideal rotor, Betz.

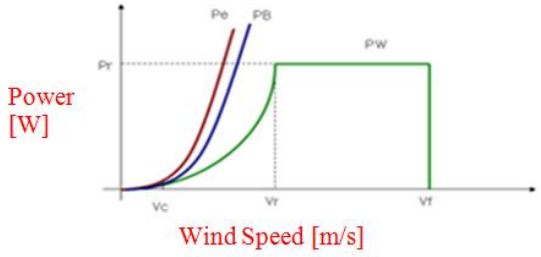

Figure 4: Graph of Output Characteristics of Wind Turbine Generator

Because wind turbines have mechanical friction and loss, the wind speed increases and the rotor rotates when the torque generated by the rotor overcomes this. At this time, the wind speed is referred to as a starting wind speed Vc, and the output of the wind power generator is referred to as a rated Pr and a rated wind speed Vr. The design wind speed of the rotor is an important parameter that determines the efficiency and economical efficiency of the wind power generation system.

Electrical Characteristics of Solar Cell

The output power of the solar cell is calculated as the product of the output voltage and the output current and is shown in the form of a parabola as shown in Figure 5[5].

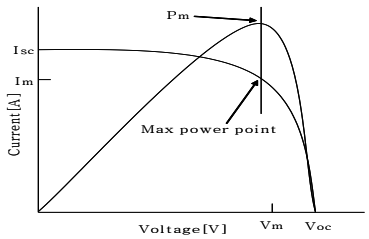

Figure 5: The Maximum Voltage of a Solar Cell and the Maximum Output Point

Further, there is a point in which the output power of the solar cell depending on the temperature becomes maximum. Figure 6 shows the operating point at which the output becomes maximum even in the current-voltage characteristic curve as the solar radiation changes[6].

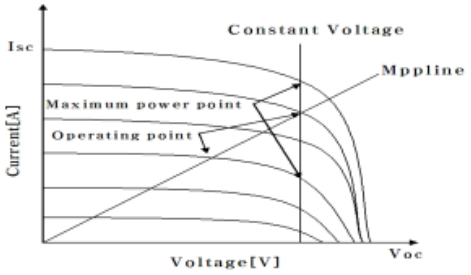

Figure 6: MPPT Solar Radiation Due to Differences

The energy distribution of solar energy is determined by each wavelength represented by the spectrum. Solar mass, solar cell surface temperature, wind velocity, air mass, transparency, turbidity, ozone layer and vapor layer thickness are also parameters that affect solar cell efficiency.

3. Design Method of Hybrid Generation System with EDLC

Configuration of Hybrid Power Generation System

Hybrid power generation combines a Plurality of systems having different characteristics to construct a power generation system complementary to each other, so that a plurality of systems can be smoothly combined, and advantages of each individual system and further advantages the purpose is to acquire. Figure 7 is an energy storage flow diagram of a hybrid power generation system. The output of the power generation system is converted to a DC output through a power converter and delivered to a common DC bus.The hybrid power generation system requires a photovoltaic power generation system that performs MPPT operation and the wind power generation system also has a variable output characteristic with varying output characteristics depending on the wind speed. Therefore, even if a separate DC / DC converter is used, Algorithm is Needed.

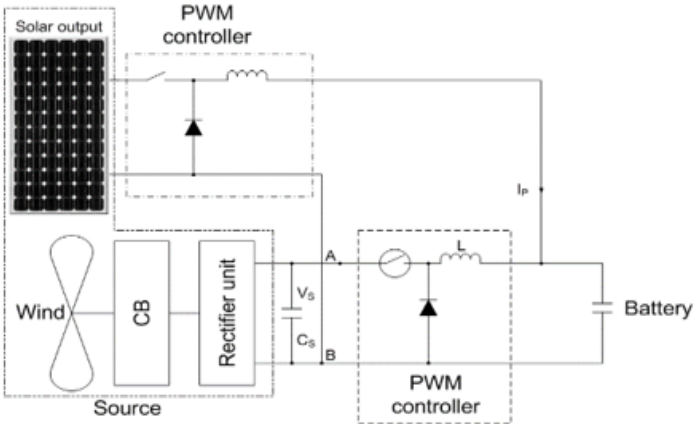

Figure 7: Energy Storage Flow Diagram of a Hybrid Power Generation System

MPPT Algorithm by Feedback

Table 1 shows that the maximum output of the solar cell modules is 144W in parallel. In STC, the MPP voltage is 60.5 [V] and the MPPT current is 4.7 [A]. The maximum power point was found by applying a solar cell module with MPPT tolerance within 3% according to the grid connection technique of the distributed power supply[3].

Table 1. Characteristics of the solar cell module

Energy Storage and EDLC

In the PV system, the battery stores the electricity generated during the daytime, and is used as an energy source when the load is larger than the power generation amount or when the power generation is impossible. The terminal voltage V at the time of charging the battery is larger than the electromotive force at the time of no-load of the battery. This is due to the internal equivalent resistance R. The remaining capacity SoC (State Of Charge) of the battery increases as the charge progresses. The value of the state of charge (SoC) can be expressed as an integrated value of time for the current as shown in equation (18).The open-circuit voltage and the internal resistance component are expressed as a function of the remaining capacity. When the charge current is i, the battery characteristics are expressed by the equation (7), and the battery characteristics can be represented by open-circuit voltage, internal resistance, variable resistance and remaining capacity component[7].

$$\mathrm{SoC} = \mathrm{SoC}_i + \int_i^{fi} Idt \tag{18}$$

Here, the remaining capacity after charging, and the remaining capacity at the beginning of charging are the charging currents. When the battery is charged, the voltage increases with the increase in the remaining capacity, and the voltage decreases when the battery discharges. Figure 8 shows the battery charge / discharge characteristics[8].

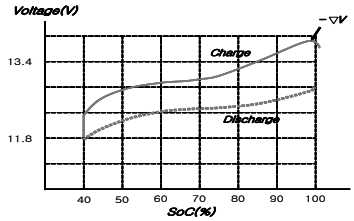

Figure 8: The Battery Charge and Discharge Characteristics Graph

the charging process, the voltage increases, but when the battery is charged, the voltage temporarily decreases due to the reverse reaction inside the battery. If the charging is not terminated, a lot of heat is generated and the battery is damaged, which shortens the battery life do.Therefore, charging must be terminated immediately. (8) and (9) are the terminal voltage of the battery.

$$V_b = R_i + V_{op} \tag{19}$$

$$V_b = ri + R_v i + F(SoC) \tag{20}$$

Where F(SoC) is a function of SoC.

Battery Capacity Estimation

The most important factor in estimating the capacity of the battery is the size of the load and the available solar energy during the period when the solar cell does not develop. In the case of domestic weather conditions, the case where the

effect of rainy season or snowfall is the longest is selected as the longest day. Since it is unlikely that it is more than 3-4 days, it is generally calculated as 4 days.The battery capacity is calculated by the formula of (21) as the product of the battery power, the current consumption per day, the discharge depth, and the margin of the battery[9,10].

$$B_w \times \eta_b \times B_{DOD} = N_d \times L_a \quad (21)$$

Where is the battery capacity, is the boil-off, is the battery efficiency, daily used power, and battery discharge depth (0.6-0.7).The amount of current used per day is divided by the voltage and the efficiency considering the load and the use time, and is expressed by Equation (22).

$$L_a = \frac{L_w \times H_a}{V_b \times \eta_i} \quad (22)$$

Here, the use time, the battery voltage, the system efficiency, and the load amount. The actual battery capacity calculation formula is shown in Equation (23).

$$B_w = \frac{N_d \times L_w \times H_a}{V_b \times \eta_i \times \eta_b \times B_{DOD}} \quad (23)$$

4. Implementation and Performance Evaluation

Characteristics of Supercapacitors

EDLC is prepared to convert electric power generated from battery replacement and photovoltaic power generation into AC through an inverter to be connected to the system, or utilize direct current even if it is used for ESS and electric vehicle charging.Figure 9 is a graph showing the energy storage density when the secondary battery and EDLC are used at the same time. [11,12].

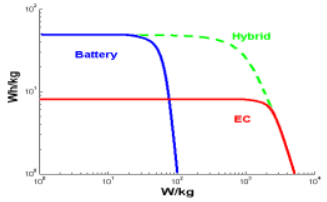

Figure 9: Batteries, EDLC and the Energy Storage Density and Hybrid

The Voltage Balance Circuit of the EDLC

The voltage profile of the EDLC has two components: a capacitive component and a resistive component. The capacitive component represents a change in voltage due to the variation of energy, and the resistance component refers to a voltage variation by an equivalent series resistance ESR (Equivalent Series Resistance).Figure 10 shows the discharge profile of a supercapacitor[13].

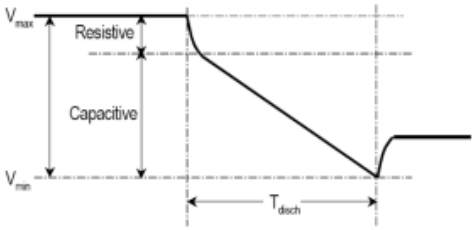

Figure 10: A Constant Current Discharge Profile of the Super Capacitor

In Fig. 10, the variable V_{max} is the operating voltage, the resistive (ESR) is the voltage drop due to the ESR, and the capacitive is the voltage drop due to the discharge of the capacitor. Vmin is the minimum voltage due to the minimum voltage during the system or discharge time, and Tdsch means the discharge time, respectively. The capacitive component is determined by equation (24).

$$i = \mathrm{C} \times \frac{dV}{di} \tag{24}$$

Where I is the current, C is the capacitance, dV is the variation of the voltage, and dt is the variation of time. The resistance component is also determined by equation (25).

$$\mathrm{V} = i \times \mathrm{R} \tag{25}$$

Where V is the voltage drop of the resistor, I is the current, and R is the ESR.

Hybrid Generation System Output

Prediction of Power Output of Hybrid Power Generation System

The probabilistic density Function of wind speed and solar irradiance is determined based on the past climate data and the probability density function of wind speed and solar irradiance and the parameters of PV arrays and wind turbines are compared with those of combined power generation system It is used to calculate the average generated power and selects the optimal solar array and wind power capacity for load fluctuation.Since the magnitude of wind speed and solar radiation is random data, it is appropriate to apply statistical parameters for solar and wind power generation factors by statistical calculation method. Figure 11 shows the annual average solar irradiation and solar cell yield.

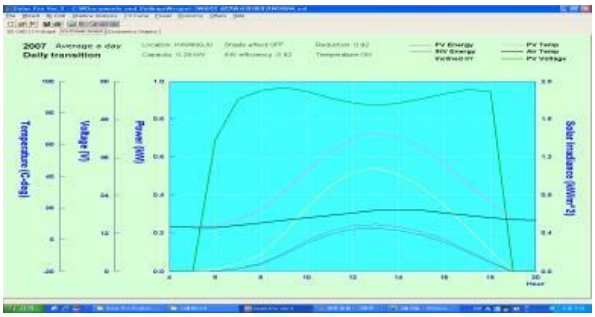

Figure 11: Graph of Annual Solar Irradiation and Solar Cell Output

Simulation for the design of hybrid power generation system was made using HOMER (the hybrid optimization model of electric renewable) program developed by US National Renewable Energy Laboratory. Figure 12 shows the simulation execution screen of the simulation program HOMER.

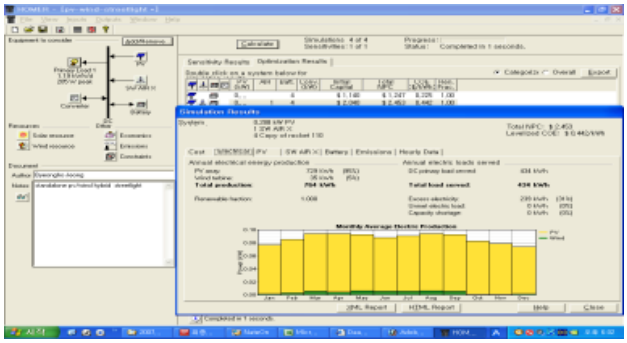

Figure 12: Monthly Solar Radiation and Solar Cell Yield Graph

Parameters such as solar radiation, wind speed, load, converter efficiency, etc. are required to perform hybrid power generation system simulation. The solar radiation and wind data required for the calculation of the solar power generation system were utilized by the data of 2007 Kwangju Regional Meteorological Agency.As a result of simulation, 95% of 764KWh of total power generation is generated in PV system and the remaining 5% is developed in wind power generation system. As a result of the simulation, an excess power generation of 239 KWh is generated, so that the ratio of load to system is appropriate.

Battery Capacity Estimation

In order to minimize the capacity of the battery in the hybrid power generation system, the capacity of the battery is selected so that the surplus power can be stored at the maximum. The battery capacity calculation can be expressed as a product of the battery power efficiency, the daily consumption current, the discharge depth, and the battery margin. The capacity of the battery in a stand-alone PV system is expressed by

$$B_w \times \eta_b \times B_{DOD} = N_d \times L_a \tag{26}$$

$\eta_b$is Battery efficiency, B_{DOD}battery discharge depth (0.6 ~ 0.7), and Boil-off, are expressed in daily use current. The amount of current used per day is expressed by the value divided by the voltage and efficiency considering the lighting capacity and the operating time(27).

$$L_a = \frac{L_w \times H_a}{V_b \times \eta_i} \tag{27}$$

Where is the average usage time, is the battery voltage, is the system efficiency, and is the load. The battery capacity is calculated as shown in equation (28).

$$B_w = \frac{N_d \times N_w \times H_a}{V_b \times \mathfrak{n}_i \times \mathfrak{n}_b \times B_{DOD}} = \frac{L_a \times N_d}{B_{DOD} \times \eta_b} \tag{28}$$

When the actual calculation is carried out, the battery discharge depth of lead accumulator is = 0.6. Calculate the day of the week defined as a day in which there is no or no wind, = 2 days. The battery voltage is = 24V, and the system efficiency of the charging circuit is 0.8, which is 80%. The load is about 41Ah when the daily usage is 1,000W and the voltage 24V is used and multiplied by the margin. Average use time = 10 hours. Battery efficiency is set to 0.9 on average. The battery capacity is given by equation (29).

$$B_w = \frac{N_d \times L_w \times H_a}{V_b \times n_i \times n_b \times B_{DOD}} = \frac{L_a \times N_d}{B_{DOD} \times \eta_b} = \frac{52Ah \times 2day}{0.6 \times 0.9} = \frac{104}{0.54} = 192Ah \quad (29)$$

The battery capacity in the above calculation is the minimum capacity required. When the DC link voltage rises, the upper limit of the voltage is set. When the voltage rises due to power unbalance occurs, the dump load is connected to the common dc link, The function of buffering action should be added.

System Capacity Setting of Hybrid Power Generation Facilities

In designing a hybrid power generation system, it is essential to design a stable system that can accommodate the demands of the load with the minimum cost. Since this system applies a standalone streetlight load, the load is concentrated at night. In addition, the characteristic of LED lighting consumes very stable power, so it is easy to calculate load stability.

System capacity design of hybrid power generation system is firstly selected based on daily load. In the case of stand-alone streetlight, it can be calculated by averaging over a period of 10 hours. The output power generation based on the daily data on the annual average of the combined power generation system is shown in Equation (30).

$$P_a(t) = N_{wind}P_{wind}(t) + N_{PV}P_{PV}(t) \quad (30)$$

Where is the daily output by the average annual data of the combined power generation system, and is the number of wind turbines and the number of solar cell modules. And is the electric power generated from the wind power generation and solar power generation at time t. Equation (31) represents the number of solar cell modules and the number of wind power systems for the total load L, respectively.

$$P_o \cdot \eta_\omega = L \quad (31)$$

$$W_o \cdot \eta_\omega = V_i \quad (32)$$

Where W is the number of wind power systems that meet the total load L, PV is the efficiency of the wind power generation system, Po is the sum of the power generation of the independent PV system, Wo is the independent It is the sum of the amount of development of the wind power generation system.

Figure 13 shows the photovoltaic output voltage and current waveforms through actual applied system, and Figure 14 shows the wind power output voltage and current waveforms.

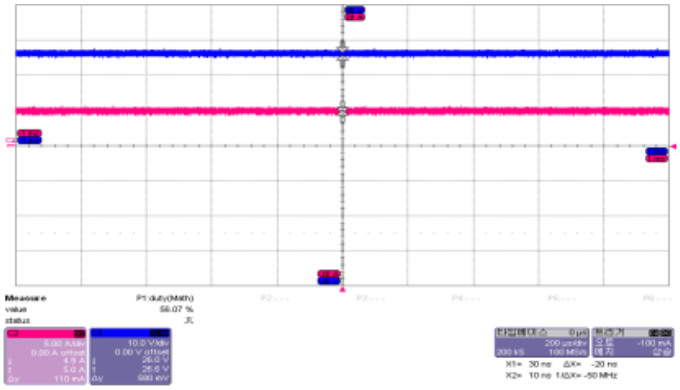

Figure 13: PV Output Voltage and Current Waveform

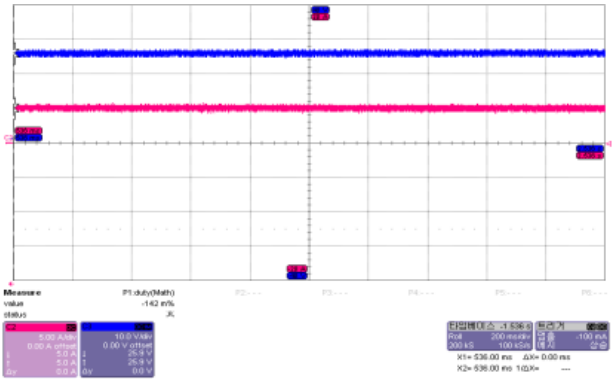

Figure 14: Wind Power Output Voltage and Current Waveform

As can be seen in Figures 13 and 14, it can be observed that the current and voltage are converted to DC, and the battery is charged according to the current meteorological conditions and charged with the battery's charge voltage and current.

5. Conclusion

In this study, we need battery storage technology of surplus energy of solar - wind power hybrid independent power generation system. Balancing control technology was designed, fabricated and experimented to secure high voltage and constant current drive design technology for high power LED lighting device using technology using super capacitor.

In sunny weather, wind power was found to increase in the windy cloudy weather. If such hybrid type of power is produced, it is possible to reduce the pulsation of the total production power, so that it can supply stable power to the load system.

Future Research Projects Design of solar-wind power hybrid power generation system which is advanced in conjunction with condensed solar cell module by reflecting the influence of progressive power charge according to power charge

and total accumulated load power varying by time, Standardization is promoted to establish technology.

Thanks to that: This study was conducted with the support of Gwang-ju University Research Fellows in the 2017 academic year.

References

[1] Jung Y., Kim D., Cho N., AVR Atmega128A Bible, BOGDOO, (2013), 200-216.

[2] Ruther R., Montenegro A., Salamon A., Araujo I., The Petrobras 45.5kwp, gridconnected PV System: a Comparative Study of Six Thin-film Module Types Operating in Brazil , Proceedings of the 29th IEEE Photovoltaic Specialists Conference (2002), 1440-1443.

[3] Noh H.J., Lee D.Y., Hyun D.S., An Improved MPPT Convertor With Current Compensation Method for Small Scaled PV-Applications, IEEE IES 2 (2002), 1113-1118.

[4] Huh H., Lee J., A Study on Development of H8 MCU IDB(Integrated development board) for Embedded Education, J. of The Korea Institute of Electronic Communication Sciences 4(1) (2009), 51-57.

[5] Wang M., Nehri M., Nelson D., A simulink-based model for a stand-alone wind-photovoltaic/fuel cell generating system, Proc. of the NAPS, Texas A&M University, College Station; TX (2001).

[6] Andoubi R., Mami A., Annabi M., Bond Graph Modelling and Dynamic Study of a Photovoltaic System Using MPPT Buck-Boost Converter, IEEE ICS 3 (2002), 200-205.

[7] Mohan N., Robbins P., Power Electronics:Converters, Applications and Design, Willey, Third Edition (2003), 161-173.

[8] Kim H., Development of d stand-alone solar street light controller integrated, J. of the Korea Institute of Electronic Communication Sciences 7(6) (2014), 641-647.

[9] Im J., Choi J., Song S., Lee D., The Design of Digital Controller for Boost Converter on Photo-Voltaic System, J. of the Korean Solar Energy Society 30(6) (2010), 22-27.

[10] Kim S., Lee K., Implementation of Successive Approximate Register Typed A/D Converter for a Monitored Battery Voltage Conversion, J.of the Korea Institute of Electronic Communication Sciences 6(2) (2011), 256-261.

[11] Jung Y., A Study on Generalized Output Capacitor Ripple Current Equation of Interleaved Boost Converter, J.of the Korea

Institute of Electronic Communication Sciences 7(6) (2012), 1429-1435.

[12] Jung Y., Input Ripple Current Formula Analysis of Multi-Stage Interleaved Boost Converter, J. of the Korea Institute of Electronic Communication Sciences 6(6) (2011), 865-871.

[13] Shin H., Characteristics of AC-DC Converter using Multilayer Piezoelectric Transformer, J.of the Korea Institute of Electronic Communication Sciences 7(6) (2012), 1315-1320.